PHYSICAL REVIEW A **71**, 045601 (2005)

Feshbach resonances in fermionic ^{6}Li

C. H. Schunck, M. W. Zwierlein, C. A. Stan, S. M. F. Raupach, and W. Ketterle
Department of Physics, MIT-Harvard Center for Ultracold Atoms, and Research Laboratory of Electronics, MIT, Cambridge, Massachusetts 02139, USA

A. Simoni, E. Tiesinga, C. J. Williams, and P. S. Julienne
National Institute of Standards and Technology, 100 Bureau Drive stop 8423, Gaithersburg, Maryland 20899-8423, USA

(Received 14 July 2004; published 5 April 2005)

Feshbach resonances in ^{6}Li were experimentally studied and theoretically analyzed. In addition to two previously known *s*-wave resonances, three *p*-wave resonances were found. Four of these resonances are narrow and yield a precise value of the singlet scattering length. The position of the broad *s*-wave resonance near 83 mT is mostly sensitive to the triplet potential. It was previously determined in a molecule-dissociation experiment for which we, here, discuss systematic shifts.

DOI: 10.1103/PhysRevA.71.045601 PACS number(s): 03.75.Ss, 32.80.Pj, 34.50.Pi

Interactions in ultracold atomic gases can be magnetically tuned using Feshbach resonances [1]. A Feshbach resonance occurs when the energy of two colliding atoms is nearly degenerate to the energy of a bound molecular state. Tunable interactions have been used to explore novel phenomena in collisional and many-body physics. Recently, Feshbach resonances have been used to control pairing processes in ultracold fermionic gases. This led to the achievement of Bose-Einstein condensation (BEC) of molecules in ^{40}K [2] and ^{6}Li [3–5] and to the first studies of the BEC-BCS crossover, the continuous transition of fermion pairs from weakly bound molecules to long-range Cooper pairs [5–11].

Most experiments in ^{6}Li have been carried out in the vicinity of the *s*-wave Feshbach resonance near 830 G [5,7–11] ($1\text{ G}=10^{-4}\text{ T}$). The quantitative interpretation of these experiments and the characterization of the BEC-BCS crossover require a precise knowledge of the resonance location. However, its determination is not trivial since the resonance width is extremely large and the line shape is strongly affected by many-body effects. In our previous work we determined the position of this resonance by the onset of molecule dissociation to be 822 ± 3 G [8].

In this paper we report on a detailed study of Feshbach resonances in the two lowest hyperfine states of ^{6}Li with the goal of accurately characterizing the interaction potential of two ^{6}Li atoms. In addition to two previously known *s*-wave resonances, we find three *p*-wave resonances [12]. The positions of the *p*-wave resonances together with the location of the narrow *s*-wave resonance near 543 G are used for a precise determination of the singlet *s*-wave scattering length. These results, however, do not constrain the position of the broad resonance, which also depends on the triplet scattering length. An improved measurement of its location is presented and the magnitude and the origin of possible systematic errors are discussed.

The experimental setup has been described in Ref. [13]. Up to 4×10^7 quantum degenerate ^{6}Li atoms in the $|F,m_F\rangle=|3/2,3/2\rangle$ state were obtained in a magnetic trap by sympathetic cooling with ^{23}Na. The ^{6}Li atoms were then transferred into an optical dipole trap (ODT) formed by a focused 1064-nm laser beam with a maximum power of 9 W. In the optical trap a single radio-frequency sweep transferred the atoms to state $|1\rangle$ ($|F,m_F\rangle=|1/2,1/2\rangle$ at low field). A subsequent Landau-Zener sweep at an externally applied magnetic field of 565 G could then be used to either prepare the entire sample in state $|2\rangle$ ($|1/2,-1/2\rangle$ at low field) or create an equal mixture of atoms in states $|1\rangle$ and $|2\rangle$. Except for the measurement of the broad *s*-wave Feshbach resonance, all resonances were observed by monitoring magnetic-field-dependent atom losses. Atom numbers were obtained from absorption images taken at zero field. The externally applied field was calibrated by driving microwave transitions from state $|2\rangle$ to state $|5\rangle$ ($|3/2,1/2\rangle$ at low field) at several magnetic fields close to resonance positions and from state $|2\rangle$ to state $|3\rangle$ ($|3/2,-3/2\rangle$ at low field) at high magnetic fields around 800 G.

For spin-polarized samples either in state $|1\rangle$ or $|2\rangle$ *s*-wave scattering is forbidden by symmetry; therefore, the observed resonances occur in the *p*-wave channel. The same molecular state that is responsible for these two resonances also causes a *p*-wave resonance in the $|1\rangle+|2\rangle$ mixture. The three *p*-wave resonances were observed in clouds with typical temperatures $T\sim6\ \mu$K and $T/T_F\simeq0.5-1.5$, where T_F is the Fermi temperature. Radial and axial trap frequencies were typically $\omega_r=2\pi\times1.0$ kHz and $\omega_a=2\pi\times6.9$ Hz.

The position of the *p*-wave resonance in the collision of a pair of state $|1\rangle$ atoms was determined by first ramping the magnetic field to approximately 5 G below the resonance. Using an additional power supply to precisely change the magnetic field within a 10 G range, the field was then switched in 1 ms to a test value B_{test}. Here the atoms were kept for 200 ms before the field and the optical trap were switched off. Finally, atom number versus B_{test} was recorded. Resonantly enhanced losses due to inelastic three-body decay led to a Lorentzian shaped feature as shown in Fig. 1(a). Resonance positions and widths are summarized in Table I.

The same technique was used to determine the $|1\rangle+|2\rangle$ and $|2\rangle+|2\rangle$ *p*-wave resonances. The resonance line shapes are asymmetric (see Fig. 1), possibly due to threshold effects [14,15]. The splitting of a *p*-wave resonance due to spin-spin interactions [16] is for these resonances more than one order

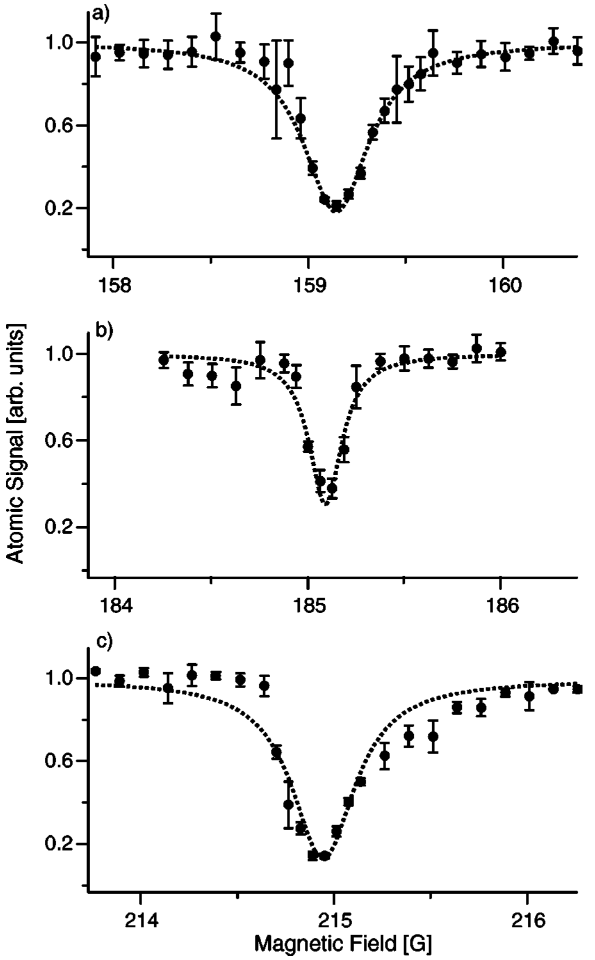

FIG. 1. p-wave resonances for $|1\rangle+|1\rangle$ (a), $|1\rangle+|2\rangle$ (b), and $|2\rangle+|2\rangle$ (c) collisions. Dashed lines are Lorentzian fits to the data. The results are summarized in Table I.

TABLE I. Position of the Feshbach resonances. Given are the experimentally and theoretically determined resonance locations B_{expt} and B_{theory}, respectively, and the measured resonance width. The uncertainties for the experimental data in the first four rows are dominated by magnetic field drifts between the measurement of the resonance and the field calibration for which we find an upper bound of 80 mG. For the $|1\rangle+|1\rangle$ resonance an additional drift was monitored. The statistical error of determining the line center and the estimated uncertainty due to asymmetric line shapes are negligible. The quoted linewidths are not corrected for source depletion due to atom loss. We estimate that this effect reduces the linewidths by 25%–40%. For the broad s-wave resonance (fifth row) only a range is given. See the text for a discussion.

States	Wave	B_{expt} [G]	B_{theory} [G]	Width [G]
$\|1\rangle+\|1\rangle$	p	159.14±0.14	159.15(4)	0.4
$\|1\rangle+\|2\rangle$	p	185.09±0.08	185.15(4)	0.2
$\|2\rangle+\|2\rangle$	p	214.94±0.08	214.90(4)	0.4
$\|1\rangle+\|2\rangle$	s	543.28±0.08	543.27(5)	0.4
$\|1\rangle+\|2\rangle$	s	822…834		

of magnitude smaller than the width and could not be discerned with our sensitivity.

The position of the s-wave resonance near 543 G in the $|1\rangle+|2\rangle$ mixture was determined as presented above in clouds with typical temperatures of 6 μK, but in a slightly deeper optical trap and with an extended holdtime of 2900 ms at B_{test}. The result of a fit to the Lorentzian lineshape is given in Table I. This s-wave resonance was first reported in [17] and calculated in [18].

To determine the position of the broad s-wave Feshbach resonance near 830 G a different method was required. The resonance was identified as the onset of molecular dissociation [6,8,19]. Molecules were first created on the repulsive (BEC) side of the Feshbach resonance and then dissociated into atoms when the magnetic field crossed the resonance. However, this method is subject to systematic shifts in the resonance position that depend on the molecular density and the speed of magnetic field ramps. To control the density-dependent shift, the molecular density was varied by using different parameters for the optical dipole trap and by performing the dissociation at different times of flight.

The starting point of the experiment was an almost pure $^6Li_2$ molecular BEC that was prepared at a magnetic field of about 780 G in the optical trap as described in Ref. [8]. The data shown in Fig. 2 were obtained by releasing the molecules from the optical trap at 780 G [20]. After 2 ms the field was ramped to a test value B_{test} in 14 ms. In these first 16 ms time of flight the peak molecular density dropped by three orders of magnitude to $n_{\text{mol}}=5\times10^9\ \text{cm}^{-3}$. The magnetic field was held at B_{test} for another 5 ms before it was ramped down. The critical field ramp, which can alter the resonance position, is the initial phase of the magnetic field ramp down in which the molecules are still in the resonance region. Here, fast ramps can dissociate weakly bound molecules. However, we could only use a limited time of flight while maintaining a good signal-to-noise ratio. Therefore the field was ramped down in two steps: at an initial rate of 100 G/ms for 2 ms to leave the resonance region, followed by an exponential decay with time constant 30 G/μs which brought the field to zero in 3 ms. To better control the effects of the field ramp, the experiment was repeated for different initial switch off speeds. Finally, the sample was imaged with light which was resonant only with unbound atoms; the possible molecular transitions are far detuned from the atomic transition at zero field. By monitoring the atom number as a function of B_{test} the onset of molecule dissociation was observed. The data in Fig. 2 show the onset at 821±1 G. The slow approach of the atomic signal to unity reflects the time constant of dissociation and the possible reconversion of atoms into molecules during the magnetic field switch off. In our analysis only the onset of the atomic signal was evaluated.

We now consider the two sources of systematic errors mentioned above in more detail. Few-body collisions might dissociate molecules when their size, which near resonance is on the order of the scattering length between the constituent atoms [21], becomes comparable to the mean distance between the molecules, $a\sim n_{\text{mol}}^{-1/3}$. The scattering length near resonance is parametrized by $a=a_{\text{bg}}[1+\Delta B/(B-B_0]\approx a_{\text{bg}}\Delta B/(B-B_0)$, where a_{bg} is the negative background scat-

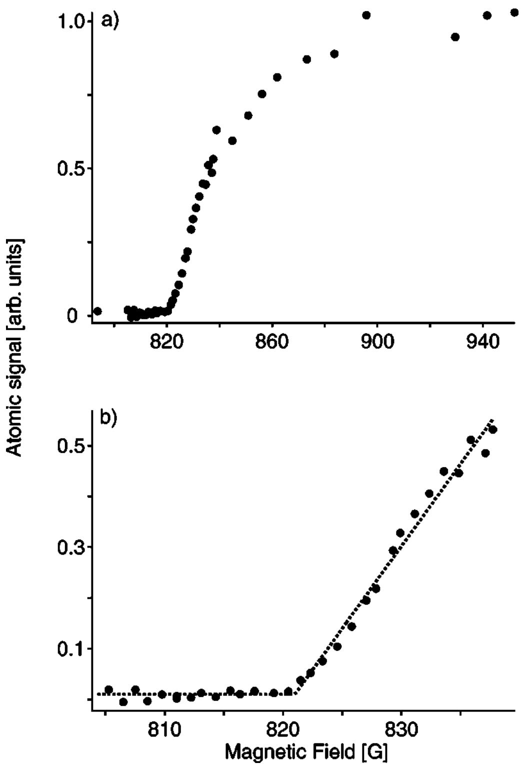

FIG. 2. Determination of the position of the broad *s*-wave Feshbach resonance. (a) Onset of dissociation of molecules into atoms at 821±1 G. (b) The resonance position was obtained by fitting two lines to the data points near the threshold, one horizontal through the points showing no atomic signal and a second line following the initial rise in atom number. The intersection of the two lines gives the resonance position; the estimated uncertainty of this point is ±1 G.

tering length, B_0 is the resonance position, and ΔB is the resonance width. So molecule dissociation will become important at a magnetic field B for which $a_{\mathrm{bg}}\Delta B/(B-B_0) \sim n_{\mathrm{mol}}^{-1/3}$. For the broad resonance, this density-dependent, few-body effect is expected to shift the observed resonance position to lower magnetic fields.

The second systematic error is a density-independent, single-molecule effect. Switching off the magnetic field becomes nonadiabatic close to resonance and destroys very weakly bound molecules [22]. If a molecule with binding energy $\hbar\omega=\hbar^2/(ma^2)$ is forced to change its size faster than its oscillation frequency (i.e., if $\dot{a}/a \gg \omega$), the molecule may dissociate. With the magnetic field dependence of a given above, the rate $\dot{a}/a \sim \dot{B}/(B-B_0)$ becomes comparable to $\omega \sim (B-B_0)^2$ at a magnetic field that is shifted from the resonance location B_0 by $\Delta B=B-B_0 \sim \dot{B}^{1/3}$. This expression gives the scaling of the ramp-induced systematic error with the ramp speed $\dot{B}$.

To find the order of magnitude of these shifts we have determined the resonance locations for three different ramp rates at constant density and for three different densities at constant ramp rate.

At a molecular density of $n_{\mathrm{mol}}=1.5\times 10^{10}$ the resonance positions were measured at initial ramp speeds of 30 G/μs (fastest possible switch off), 100 G/ms (fastest externally controlled ramp), and 12.5 G/ms (controlled ramp). For the fastest switch off the onset of dissociation occurs at 793±7 G, for the other two controlled ramps at 822±3 G. Assuming that no density shifts affect these data, one can extrapolate to zero ramp speed based on the $(B-B_0) \propto \dot{B}^{1/3}$ dependence. In this way we find a resonance position of 825±3 G.

For a fixed initial ramp speed of 100 G/ms the resonance locations were determined at densities of 5×10^9 cm^{-3}, 1.5 $\times 10^{10}$ cm^{-3}, and 1.2×10^{12} cm^{-3} to be 821±1 G, 822±3 G, and 800±8 G, respectively. Here one can use the $(B-B_0) \propto n^{1/3}$ dependence to extrapolate to a resonance position of 825±3 G, neglecting effects due to nonadiabatic magnetic field ramps.

Both systematic effects shift the maximum magnetic field value at which the molecules are stable to lower magnetic fields. In a simple picture, one would expect the total shift to be the larger of the two. However, if they are similar, as in our case, they may add or combine in a more complicated way. We have measured the threshold position at low density and slow ramp rates to be 822±3 G and determined two shifts of 3±3 G. Therefore, we expect the position of the Feshbach resonance to be between 822 and 834 G. A more accurate extrapolation requires measuring the dissociation threshold for more ramp speeds and densities. However, technical limitations in varying magnetic field ramp speeds and an unfavorable signal-to-noise ratio at lower densities precluded this.

All Feshbach resonances discussed in this paper are due to the $v=38$ vibrational state of the singlet potential with total electronic spin S equal to zero. The p-wave resonances have a total nuclear spin $I=1$, while the 543 G and broad s-wave resonances have $I=2$ and $I=0$, respectively.

The resonance locations are compared with results of scattering coupled-channel calculations. We locate the resonance from the maximum of the elastic cross section as a function of magnetic field. The collision energy is fixed at $E=k_BT$, where k_B is the Boltzmann constant and T is the experimental temperature. Our collision model, described in detail in Ref. [18], treats the singlet and triplet scattering lengths as adjustable parameters. The triplet state has a total electron spin equal to one. It turns out that all narrow resonances, which could be accurately located, are insensitive to the triplet scattering length. Only s- and p-waves are included in the calculation. Fitting the singlet scattering length a_S to the field locations given in the first four rows of Table I yields a very accurate value of $a_S=45.1591(16)a_0$, where $a_0=0.052\,917\,7$ nm. With this value, the resonance positions given in the third column of Table I were calculated at a collision energy equal to k_BT. The agreement with the experimental values is excellent. The location of the s-wave resonance is also in very good agreement with the determination of Ref. [23], 543.26(10) G.

Our theoretical uncertainties do not include contributions due to a thermal average. Moreover, there can be a discrepancy between the field values at which the observed three-body loss rate and the theoretical two-body elastic cross section are maximal. Experimental observations on ^{40}K [14] are not conclusive about the magnitude of this shift, although they suggest it is well within the linewidth of the observed loss features. As an estimate of our possible systematic error, a shift in the resonance position δ(G) will give rise to a shift from our best a_S of $(-0.0365\delta)a_0$.

The broad resonance is caused by a hyperfine-induced mixing between a singlet vibrational level and an almost-bound virtual state of the triplet potential, a situation analyzed in [24,25]. It is the virtual state that gives rise to the large and negative triplet scattering length a_T of ^{6}Li. Mixing occurs for magnetic field values above 500 G. In fact, in absence of the hyperfine mixing, the resonance would occur around 550 G. The coupling shifts the resonance by a few hundred gauss. For typical Feshbach resonances, these shifts are no more than a few gauss. A consequence of the large shift is that the resonance location depends critically on the less well known triplet potential.

In conclusion, we have found three *p*-wave Feshbach resonances in ^{6}Li. Together with the narrow *s*-wave resonance they give a precise value of the singlet scattering length. The position of the broad resonance could not be constrained using the refined singlet potential. The determination of the position of the broad resonance via molecule dissociation is subject to systematic errors, which shift the onset of dissociation to lower magnetic fields.

The MIT research is supported by NSF, ONR, ARO, and NASA. S.R. acknowledges financial support from the Dr. Jürgen Ulderup Foundation.

[1] E. Tiesinga, B. J. Verhaar, and H. T. C. Stoof, Phys. Rev. A **47**, 4114 (1993); W. C. Stwalley, Phys. Rev. Lett. **37**, 1628 (1976); S. Inouye *et al.*, Nature (London) **392**, 151 (1998); P. Courteille *et al.*, Phys. Rev. Lett. **81**, 69 (1998).
[2] M. Greiner, C. A. Regal, and D. S. Jin, Nature (London) **426**, 537 (2003).
[3] S. Jochim *et al.*, Science **302**, 2101 (2003).
[4] M. W. Zwierlein *et al.*, Phys. Rev. Lett. **91**, 250401 (2003).
[5] T. Bourdel *et al.*, Phys. Rev. Lett. **93**, 050401 (2004).
[6] C. A. Regal, M. Greiner, and D. S. Jin, Phys. Rev. Lett. **92**, 040403 (2004).
[7] M. Bartenstein *et al.*, Phys. Rev. Lett. **92**, 120401 (2004).
[8] M. W. Zwierlein *et al.*, Phys. Rev. Lett. **92**, 120403 (2004).
[9] J. Kinast *et al.*, Phys. Rev. Lett. **92**, 150402 (2004).
[10] M. Bartenstein *et al.*, Phys. Rev. Lett. **92**, 203201 (2004).
[11] C. Chin *et al.*, Science **305**, 1128 (2004).
[12] We presented most of the results of the present paper at the KITP workshop in Santa Barbara, 2004. Similar results were independently obtained in Paris [15].
[13] Z. Hadzibabic *et al.*, Phys. Rev. Lett. **91**, 160401 (2003).
[14] C. A. Regal *et al.*, Phys. Rev. Lett. **90**, 053201 (2003).
[15] J. Zhang *et al.*, Phys. Rev. A **70**, 030702(R) (2004).
[16] C. Ticknor *et al.*, Phys. Rev. A **69**, 042712 (2004).
[17] K. Dieckmann *et al.*, Phys. Rev. Lett. **89**, 203201 (2002).
[18] K. M. O'Hara *et al.*, Phys. Rev. A **66**, 041401(R) (2002).
[19] T. Mukaiyama *et al.*, Phys. Rev. Lett. **92**, 180402 (2004).
[20] The ODT power was 36 mW, yielding trap frequencies of $\omega_r = 2\pi \times 690$ Hz radially and $\omega_a = 2\pi \times 12.5$ Hz axially. The axial frequency is mostly due to magnetic field curvature.
[21] T. Kohler *et al.*, Phys. Rev. Lett. **91**, 230401 (2003).
[22] J. Cubizolles *et al.*, Phys. Rev. Lett. **91**, 240401 (2003).
[23] K. E. Strecker, G. B. Partridge, and R. G. Hulet, Phys. Rev. Lett. **91**, 080406 (2003).
[24] B. Marcelis *et al.*, Phys. Rev. A **70**, 012701 (2004).
[25] E. G. M.v. Kempen, B. Marcelis, and S. J. J. M. F. Kokkelmans, Phys. Rev. A **70**, 050701(R) (2004).